21605

by Nanang Ruhyat

Submission date: 16-Aug-2023 07:29PM (UTC+0700)
Submission ID: 2146610916
File name: 21605-64386-1-CE.docx (2.84M)
Word count: 4909
Character count: 24197

Simulation of the drying air and the spray of liquid in the spray dryer chamber with Discrete Phase Material (DPM) and Discrete Random Walk (DRW) is CFD methods to analyze the drying liquid, was carried out in this study. The main problems in spray drying are, the adhesion of the material to the drying chamber walls, which causes uneven drying material. This adhesion can slowdown the drying process and reduce productivity. The design of the drying air inlet into the drying chamber becomes essential to research. Variations in the position of the drying air inlet into the drying chamber are carried out in the 3D spray dryer room to see the mechanism of the centrifugal velocity of the drying airflow, which can improve uniform mixing with flow resistance due to friction with small walls and the drying air velocity. This phenomenon is impossible to observe in experiments. A geometric model consisting of 1,054,000 meshes, in a hex mesh at the area around the nozzle and the top spot of the chamber and the remaining area covered with a tetrahedral net, was determined to predict velocity, temperature and fluid flow behavior. The first position, the dryer air inlet is at an angle from the diameter of the spray drying chamber. The second position is in the middle of the diameter of the drying chamber. The position of the first inlet produces a more even temperature contour with a more tangential velocity due to the small frictional resistance with the walls. While the second position is not recommended because the flow leads to one side of the wall and creates sticking and even material buildup. Double heated condenser can dry air at moderate temperatures, it is very effective drying products—positioning the dryer air inlet into the drying chamber achieving the economical production of high-quality products

1. Introduction

Spray-dryers have been known since 1870. Spray-dryers are generally used in the pharmaceutical, chemical, and food industries for the drying process [1]. The dryer changes the liquid phase of the material to be dried with drying air [2] into a vapor phase and then removes water vapor in the liquid material to become dry powder [3]. Dryers can reduce or eliminate microbial growth on the material by reducing the water content [4].

Several things that the researcher did before in determining dryer product quality as inlet drying temperature [5–7], Feed flow rate [8], Ambient temperature dan relative humidity [9], Feed Concentrated [9], Atomization speed [6, 10–12], Inlet air velocity and pressure operation as well as outlet temperature [13], and Droplet Diameter [14].

In addition to the seventh things above, it can also by the construction of the drying air inlet hole connected to the drying chamber to increase the effect of swirling flow in the material drying chamber.

The practical structure of the air-liquid junction mechanism, which is more efficient in producing dry powder, is urgently needed and has not been studied. Measurement of air flow, temperature, particle size and humidity in the drying chamber is very difficult and expensive to perform in large-scale dryers.

Previously, researchers had conducted experiments with double condensers from the refrigeration system [3]. The humidity of the air that will enter the heater room has been successfully reduced, so that the quantity of the product can be increased. Understanding of particle collisions in the drying chamber is important to study because it affects the quality of the final product.

3D CFD model of the agglomeration of droplets and particles in a counter-current spray-drying process has been studied [15]. experimental numerical methods in kinetic drying show similar results [16]. The CFD is software that can be used to predict drying phenomena in numerical analysis, as many researchers have done [1, 3]. For turbulent and economical model analysis, CFD analysis with k-ε is used [14], while to predict a more accurate flow field in the spray dryer process, the RSM method is used [15, 16]. Discrete Phase Material (DPM) is a model of material particles in the form of a ball, as a droplet or bubble followed by a type of impact, as Discrete Random Walk (DRW) methods that will occur between the material particles and the walls designed in the simulation.

In order to increase the efficiency of the drying process in the drying chamber, the effect of the position of the drying air inlet into the drying chamber will be investigated.

Spray drying is the process of converting

liquid food into a dry particulate form by spraying the food material into a hot drying medium. It provides an overview of the spray dryer machine with a combination of heating from the heater and exhaust heat from the condenser in the refrigeration system.

The spray dryer machine with a combination of heating from the heater and exhaust heat from the condenser in the refrigeration system has answered concerns about the effect of high ambient air humidity when drying materials. Dry air with low humidity can increase the flow rate of compressed air. Increasing the drying airflow rate in the drying chamber can reduce the mean spray droplet size [15]. This method is better than shrinking smaller particles. Because as the particles shrink, a narrower spray cone is formed, and air may not penetrate the center of the spray pattern until the droplet has traveled a considerable distance from the nozzle. This reduces the mixing of the material with the hot air, thereby reducing the drying rate.

Although modifications to the spray dryer as described above have been made, the quality of the product is greatly influenced by the drying conditions. The thermal damage to the product during direct drying is highly proportional to the drying temperature and the residence time of the particles in the drying chamber. In addition, droplets and dry powder adhere to the dryer wall due to the drying solution containing sugar [7]. Adhesion and subsequent deposition of the material on the surface of the dryer are still considered one of the severe problems encountered in industrial spray drying.

Various means of dealing with such products have been investigated over the years, such as the addition of a drying aid (maltodextrin), cooling the walls of the drying chamber, and the entry of atmospheric air near the bottom section, enabling the transport of powder to a collector that has atmospheric humidity. Authors [8] modified the jacketed wall for air conditioning, but it caused an increase in the relative humidity of the air close to the wall surface.

The drying chamber's measurement of airflow, temperature, particle size, and humidity is tough and expensive to perform in large-scale dryers. CFD can be a helpful tool for predicting gas flow patterns and particle phenomena such as temperature, velocity, residence time, and collision position with 3D images. CFD modeling has been widely used for drying processes to study heat and mass transfer [7] simultaneously. Although the simulation of complex transport phenomena occurring in the spray dryer cannot be modeled with high accuracy, the results are still helpful to guide the design and operation of the spray dryer when combined with empirical experience. CFD method to investigate airflow patterns, temperature, and humidity profiles at various positions in the spray drying chamber. It should be noted that the drying process is controlled by two critical factors: the convection heat transfer coefficient, which is directly related to the air velocity, and the residence time into the drying chamber [19].

Previous research [2] has shown how the product quantity is increased by accelerating the drying air flow rate, then how the product does not stick to the wall by maintaining the relative humidity along the outer wall of the drying chamber. But there is an unresolved problem related to the tangential velocity of the drying air in the drying chamber which can result in a more uniform flow throughout the drying chamber and a longer residence time of ~~the~~ particles to mix with the liquid material in the drying chamber.

This study focuses more on the results of the drying simulation in the drying chamber, where two variations of the inlet from the drying air to the drying chamber are made. Analyzing the effect of two positions in order to minimizes friction with the drying chamber walls. The results can be seen in the 3D view of the drying chamber, as if done experimentally. So that it can be analyzed which parts can reduce the number of material particles attached to the wall as expected.

The aim of the study is to get the better effect of positions of the drying air inlet in the drying chamber. To achieve this aim, the following objectives are accomplished: 1. Comparing the position of the drying air inlet into the drying chamber from variations which

can create an airflow with a greater tangential velocity of rotating dryer airflow; 2. Analyzing temperature distribution between inlet position variations.

2. Materials and Methods

2. 1. Initial Data For Simulation

In the early stages of the simulation, meshing must be done after the image is created. Meshing must cover the top, bottom and middle of the spray dryer drying chamber with the appropriate netting quality. This simulation will be carried out at a constant temperature and flow rate of 60 °C and 0.003 kg/s, respectively. The temperature of 60 °C is set because it is the lowest temperature representing a safe temperature for drying food or heat-sensitive materials.

The placement of measuring points in the drying chamber is distributed in 10 simulation points, as shown in Fig. 1.

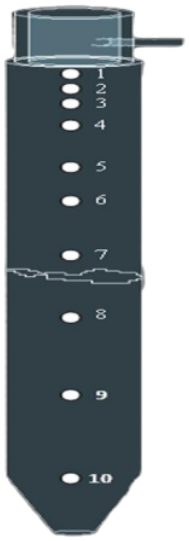

Fig. 1 Geometry mesh in the Drying Chamber

Fig. 1 and Table 1, shows the position of the temperature nodes to describe the temperature distribution in the y-direction. The node's role is described in Table 1, where the coordinate center is at the nozzle position. The position of nodes 1–4 are deliberately arranged close to each other and close to the chamber entrance to capture the quality of the mixture between dry air and spray nozzle.

Table 1
Node position of temperature in y direction

Node	*Y* (m)	Node	*Y* (m)
1	–0.02	6	–0.14
2	–0.03	7	–0.2
3	–0.06	8	–0.3
4	–0.08	9	–0.4
5	–0.12	10	–0.86

The geometric model for numerical analysis is shown in Fig. 2. The variation of the position of the drying air inlet into the drying chamber shows variations 1 and 2 at the top and bottom of Fig. 2. It shows the 3D space of the spray dryer, where the droplets interact with the air. Dryer. Overall, the geometry consists of 1,054,000 mesh counts. However, not all chamber areas are covered with the same type of mesh. Some places should be covered with hex mesh, especially around the nozzle and the chamber's top spot. All of the sites will be covered with a tetrahedral net.

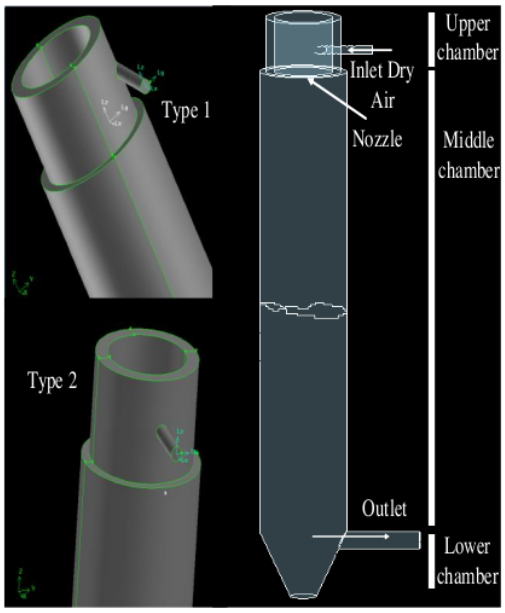

Fig. 2 Geometry model from the drying room

Furthermore, Fig. 2 shows 2 types of the position of the air duct that enters the drying chamber, namely type 1 with an inlet from the side of the drying chamber and type 2, which is a channel that enters from the center of the drying chamber.

2.2. The Equation Governing The Continuous Phase

Continuity equation:

$$\frac{\partial \rho u_i}{\partial x_i} = M_m \quad (1)$$

Momentum equation:

$$\frac{\partial \rho u_i u_j}{\partial x_i} = \frac{-\partial}{\partial x_j} + \frac{\partial}{\partial x_i} X\left[\mu\left(\frac{\partial y}{\partial x} + \frac{\partial y}{\partial x}\right) - \rho \overline{u_i' u_j'}\right] + M_f \quad (2)$$

Energy Equation:

$$\frac{\partial\left(\rho C_p u_j T\right)}{\partial x_i} = \frac{\partial}{\partial x}\left[k\frac{\partial T}{\partial x_i} - \rho \overline{u_i' T'}\right] + M_h \quad (3)$$

Ignoring the time-derived term, it's an energy storage term. The net rate of energy entering by convection. Heat conduction flows in the fluid at a certain specified distance, so that the temperature control of the distance can be seen in the form of particle momentum velocity. The value of k is the effective conductivity and T is the temperature.

The CFD code solves a system of partial differential equations with the approach taken for droplets as particles called the discrete phase model. The interaction between continuous and discrete phases will be captured using DPM in CFD code. Since there are two different phases to be simulated in the software, continuous and discrete (2006) [19], the governing equation will be explained.

2. 3. The Equation Governing The Discrete Phase

The governing the Euler-Lagrange for the trajectory of the particle, solving for the balance of forces on the particle is as follows [19]:

$$\frac{\partial u_{pi}}{\partial x_i} = C_d \frac{18\mu R_e}{\rho_p d_p 24}\left(u_i - u_{pi}\right) + g_i \frac{\rho_g - \rho}{\rho_g} + F_{xi} \quad (4)$$

The standard k– ε model uses a wall function to describe the effect of the wall the relationship between Reynolds stress and mean velocity gradien and turbulent viscosity) on the average flow (turbulent range) and shifts to a low Reynolds number formulation at low Re. The standard k–ε model can improve the accuracy of rotating flow, fast flowing tension and can also handle the problem of low Re quite well.

2. 4. Mass And Heat Transfer Between Two Phases

The evaporation rate between the particles and the hot air can be seen in the diffusion gradient in (5) and can be seen as follows [19]:

$$N_i = k_c\left(C_{i,s} - C_{i,\infty}\right) \quad (5)$$

The heat transfer between droplets and hot air can be represented as follows:

$$m_\rho C_\rho \frac{dT_p}{dt} = hA_p\left(T_\infty - T_p\right) + \frac{dm_p}{dt} h_{fg} \quad (6)$$

Several studies provide prominent comments on the use of the turbulent model. Compared to the RSM and k-ε model, using RSM, using k-ε is more economical and makes more sense. Because this model gives a slight difference in the results in terms of speed, temperature and mole fraction [20]. This simulation uses a realizable k-ε turbulent model based on ANSYS in the following.

For equation *k*:

$$\frac{\partial \rho k}{\partial t} + \frac{\partial \rho k u_j}{\partial x_j} = \frac{\partial}{\partial x}\left[\left(\mu + \frac{\mu_t}{\mu_k}\right)\frac{\partial k}{\partial x_j}\right] + G_k + G_b - \rho\varepsilon - Y_m + S_k \quad (7)$$

That G_k, G_b, are the kinetic energy of the velocity gradient and buoyancy, respectively [3]. The contribution of dilatation fluctuations incompressible turbulence to the overall dissipation rate is Y_m. S_k and S_ε are source terms.

For ε equation:

$$\frac{\partial \rho \varepsilon}{\partial t}+\frac{\partial \rho \varepsilon u_j}{\partial x_j}=\frac{\partial}{\partial x}\left[\left(\mu+\frac{\mu_t}{\mu_\varepsilon}\right)\right]+\rho C_1-\rho C_1\frac{\varepsilon^2}{k+\sqrt{\nu\varepsilon}}+C_{1\varepsilon}\frac{\varepsilon}{k}+C_{1\varepsilon}\frac{\varepsilon}{k}C_{1\varepsilon}G_b+S_\varepsilon \quad (8)$$

$$C_1=max\left[0.43\frac{\eta}{\eta+5}\right],\ \eta=S\frac{k}{\varepsilon},\ s=\sqrt{2S_{ij}S_{ij}} \quad (9)$$

The value $C_{1\varepsilon}$ $C_{3\varepsilon}$ is a constant defined in ANSYS FLUENT. One of the salient features for the k-ε realizable model is that the production of k does not involve, so the terms G_k are not the same. The difference between the k-ε and k-ε realization models is the destruction term (second term on the right) in (8). The denominator of the destruction term is never zero, but the value of k is minimal. For all these cases, the k-ε realizable model is better than the k-ε attainable model.

Simulations were carried out under steady conditions. The turbulent model used is k-ε realizable, using DPM (*Discrete Phase Model*) and DRW (*Discrete Random Walk*) to capture the interaction between continuous and discrete phases. For speed-pressure coupling scheme in this simulation is simple. There are several assumptions involved, including the chamber wall is adiabatic, so there is no energy transfer between the wall and the environment, the friction between the droplets and the wall is relatively small, and the distribution of the spray dryer on the nozzle using a rosin-rammler [18–20].

Simulations were carried out under steady conditions. The turbulent model used is k-ε realizable, using DPM (*Discrete Phase Model*) and DRW (*Discrete Random Walk*) to capture the interaction between continuous and discrete phases. For speed-pressure coupling scheme in this simulation is simple. There are several assumptions involved, including the chamber wall is adiabatic, so there is no energy transfer between the wall and the environment, the friction between the droplets and the wall is relatively small, and the distribution of the spray dryer on the nozzle using a rosin-rammler.

The DRW Model is a method to predict particle trajectories based on statistics. This calculation uses a stochastic approach that can be run based on the number of definitions in the simulation. In general, the DRW formula is given in (10) in integral time.

$$T=\int_0^\infty \frac{u'_p(t)\,u^t_p(t-\tau)}{\overline{u'^2_p}}d\tau \quad (10)$$

For equation (10) shows a proportional relationship between particle dispersion because the greater the value of T, the greater the flow turbulence. When the particle tracer is on a small scale, (10) will turn into a time integral as follows:

$$T_L=C_L\frac{k}{\varepsilon} \quad (11)$$

$$T_L\approx 0.3\frac{k}{\varepsilon} \quad (12)$$

The C_L value will be determined in a turbulent model, such as using the k-ε model shown in the following equation:

The computational model considered is standard k–ε model. The resolution of the mesh around the wall depends on the model used in the simulation.

3. Results and Discussion

3.1. Research Results Of Effet Inlet Position In Drying Quality

The results of this study are divided into two parts which show the difference in the quality of Tangential Velocity and temperature distribution. These two values are indicators that the drying carried out shows some results that shown quality improvement in drying effect.

3.2. Tangential Velocity

From the simulation results performed tangential velocity shows that effect of position drying air inlet into the drying chamber to an airflow with a greater tangential velocity of rotating dryer airflow. The velocity contours of the axial plane variations 1 and 2 are shown in Fig. 4. The air velocity of the dryer and the spray nozzle initially has a significant effect near the inlet. It gradually decreases as it gets further away from the inlet due to pressure loss and friction near the wall. In variation 2, the

decrease in speed is more significant than variation 1. The speed in the middle room is lower because it has more excellent resistance. That is, variation 2 has a greater resistance in the axial position. The resistance of variation 2 arises from friction of the walls and the collision of dry air with the middle wall in the upper chamber.

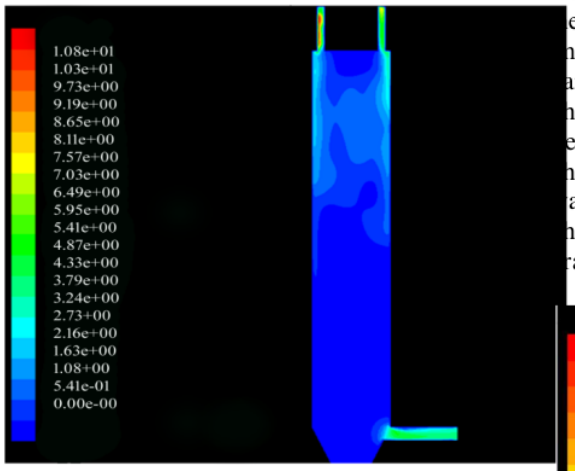

a

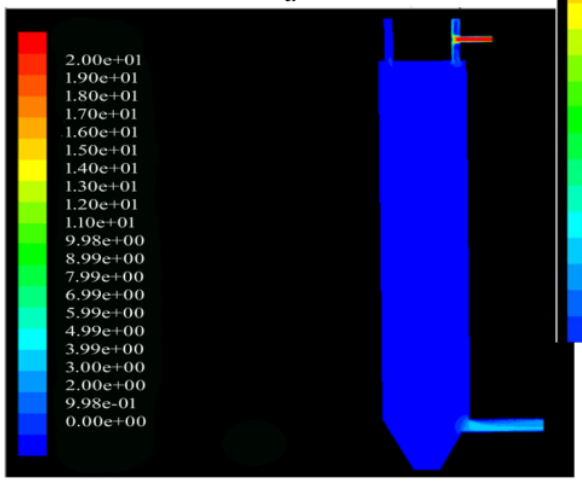

b

Fig. 3 Velocity contour at an axial position : *a* – inlet from the side of the drying chamber; *b* – duct entering from the center of the drying chamber

At Fig. 3 velocity contour at variation 2 is more homogenic than variation 1, the tangential velocity will fade at the outlet due to pressure loss and friction near the wall. Fig. 5 shows the tangential velocity that appears in the drying chamber. It shows the same result as Fig. 3. That the tangential velocity will fade at the outlet due to pressure loss and friction near the wall. Comparison of the tangential velocity vectors between variations 1 and 2 at the same eight shows that the vector in variation 1 is nore significant than in variation 2. This angential velocity causes the dry air to reach he diameter of the drying chamber and is esponsible for producing a rotating flow hroughout the drying chamber. That is, ariation 1 has a more significant vortex motion han variation 2. This will be seen in the rajectory of the particle.

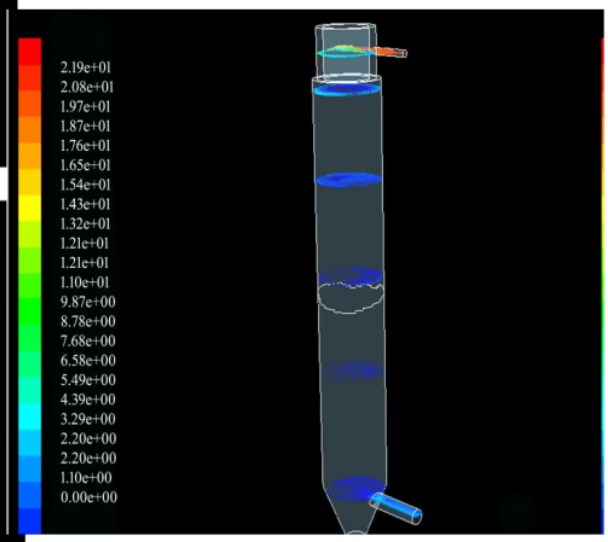

a

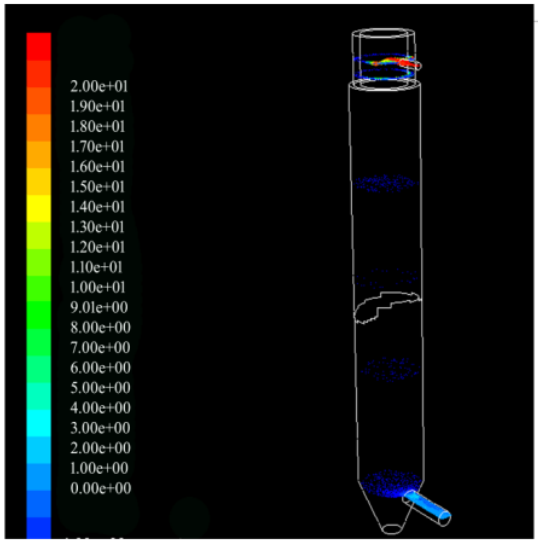

b

Fig. 4. Velocity vector along with the chamber of spray dryer in radial position: a. velocity contour at an axial position : *a* – inlet from the side of the drying chamber; *b* – Inlet from the center of the drying chamber

Comparison of the tangential velocity vectors between variations 1 and 2 at the same height shows that the vector in variation 1 is more significant than in variation 2. This tangential velocity causes the dry air to reach the diameter of the drying chamber and is responsible for producing a rotating flow throughout the drying chamber.

It can be seen in Fig. 4 that both variations 1 and 2 have secondary flows. The secondary flow in variation 1 is visible after the dry air has wholly reached the circular path in the upper chamber. Whereas in variation 2, secondary flow only appears near the inlet due to the collision of dry air against the middle wall. In variation 2, adjacent streams are pulled by an imaginary force to tend to lean to the right of the chamber.

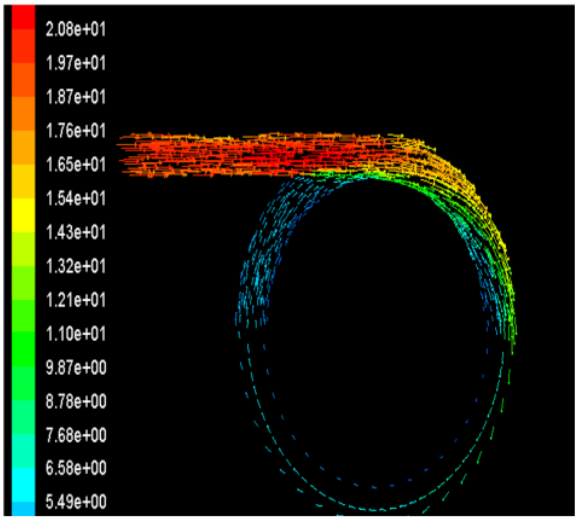

a

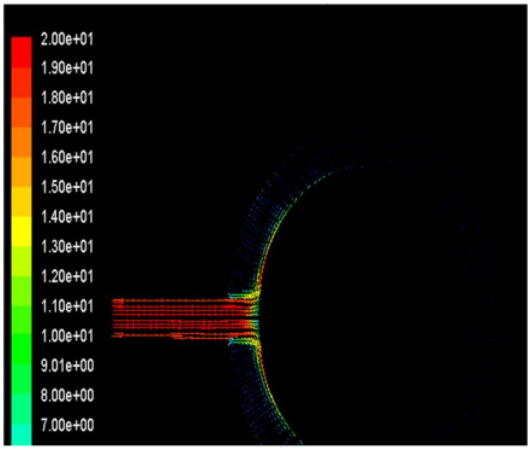

b

Fig. 5. Comparison of the velocity vector at z=0.05 in radial position : *a* – velocity contour at an axial position : a inlet from the side of the drying chamber; *b* – inlet from the center of the drying chamber

Fig. 5 shows a comparison of variations 1 and 2 in the trajectory of the spray nozzle particles. In variation 1, it is seen that the trajectory of the spray nozzle particles has a more significant circular motion than variation two because the tangential velocity is as

described in Fig. 6. Therefore, it will increase the mixing process between the drying air and liquid material, and the residence time of the particles becomes longer.

While in variation 2, it has a smaller tangential velocity than variation 1, thus reducing the circular motion. Consequently, the quantity of drying products is less, and the residence time will be faster.

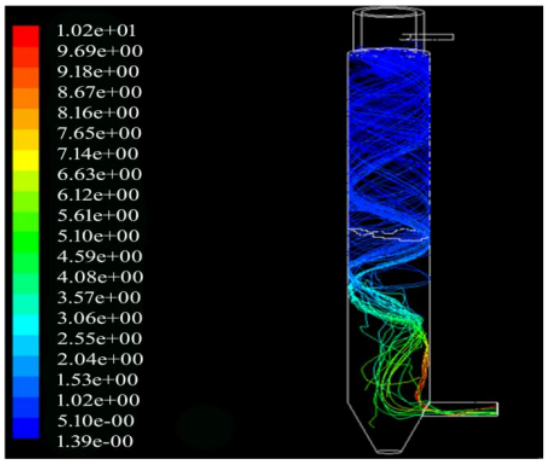

a

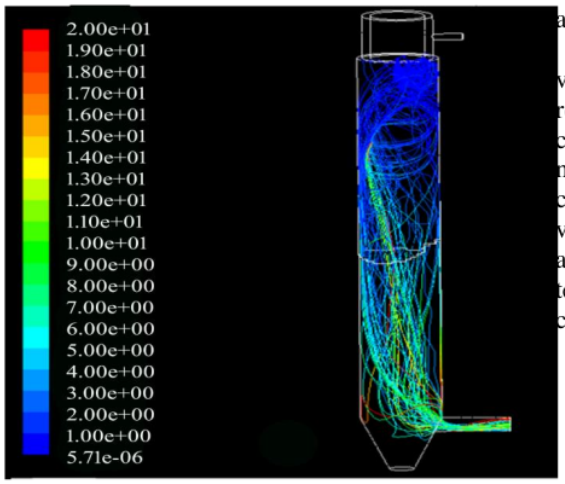

b

Fig. 6. Comparison of particle track in variation 1 and 2: *a* – inlet from the side of the drying chamber; *b* – inlet from the center of the drying chamber

Fig. 6 shows a comparison of variations 1 and 2 in the trajectory of the spray nozzle particles. In variation 1, it is seen that the trajectory of the spray nozzle particles has a more significant circular motion than variation two because the tangential velocity is as described in Fig. 5 Therefore, it will increase the mixing process between the drying air and liquid material, and the residence time of the particles becomes longer.

While in variation 2, it has a smaller tangential velocity than variation 1, thus reducing the circular motion. Consequently, the quantity of drying products is less, and the residence time will be faster.

3.3. Temperature Distribution

The temperature distribution with different inlet orientations are shown in Fig. 8. Variation 1 has a more uniform temperature than variation two due to less inhibition in the axial direction and more significant circular motion. A minor inhibition in variation one will have a more incredible axial velocity and circular motion, which supports the mixing process between dry air and nozzle spray.

Meanwhile, the temperature contour of variation 2 is not uniform because of the dry air resistance in the axial position and the small circular motion. The effect is on the uneven mixing process. In addition, the impact of the collision between dry air and the middle wall in variation 2, apart from being a flow blocker, appears secondary flow near the inlet which tends to point to the right side of the drying chamber.

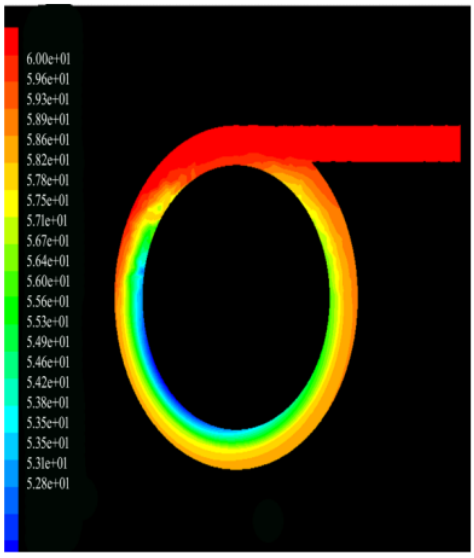

a

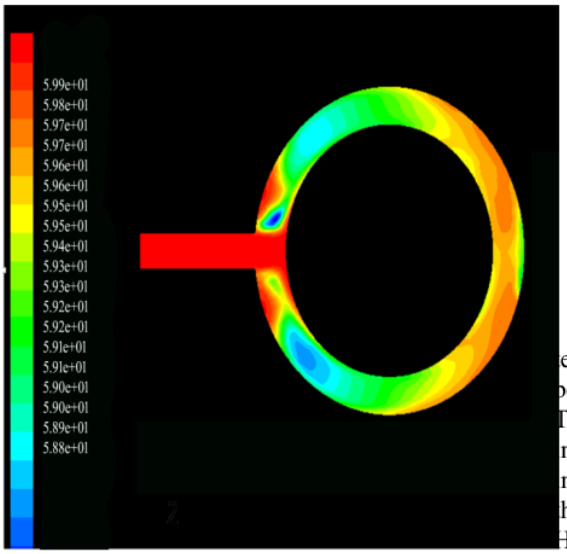

b

Fig. 7. Comparison of radial temperature contour between variation 1 and 2: *a* – inlet from the side of the dry room; *b* – inlet from the center of the drying chamber

Fig. 7 shows the radial temperature in the upper chamber. It is shown that a more incredible tangential velocity will make the radial temperature more uniform because this velocity supports dry air to flow along a circular path and reach the entire diameter of the spray drying chamber, as described in Fig. 8 This reason will answer why the radial variation of contour 2 is not uniform. This means that the tangential velocity has a significant effect on the mixing process at the radial position.

Furthermore, Fig. 8 in the graph shows how the temperature distribution in the drying chamber is.

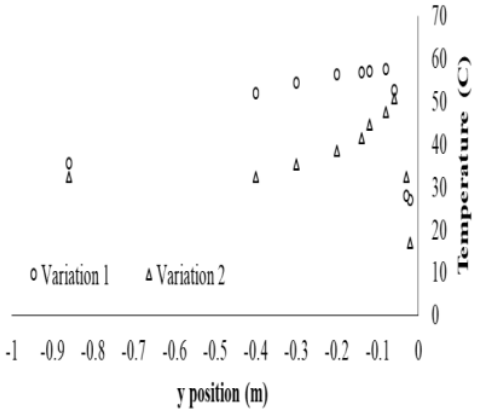

Fig. 8 Graph of Comparison distribution of temperature between variation 1 and 2

The comparison of the chamber temperature distribution along the y-direction between variations 1 and 2 is shown in Fig. 8 This indicates that temperature variation 1 increased significantly than variation 2. This implies that the quality of the mixture between the spray nozzle and the dry air is well mixed. However, getting further away from the heat source, temperature variations 1 and 2 lead to the same pattern, namely, a decrease in temperature at node 10.

3.4. Discussion Of Experimental Results Of Effect Inlet Position In Drying Quality

The placement of the inlet in variation 2 is very inefficient, where the inlet in the middle provides a large flow resistance. The radial velocity image shows that the flow resistance in

variation 1 is smaller than variation 2. So it has a better radial velocity than variation 2, as a result, variation 1 has better mixing. As seen in Fig. 4. The velocity contours of the two positions initially have a significant effect. significant near the inlet. However, it gradually decreases because it is further away from the inlet and the pressure decreases, besides that friction occurs near the walls of the drying chamber. In variation 2, the decrease in speed is more significant than variation 1. It means that variation 2 has a greater resistance in the axial position. The resistance of variation 2 arises from the friction of the walls and the collision of dry air with the middle wall from the upper room. And Fig. 5. shows the tangential velocity will fade at the outlet due to loss of pressure and friction near the wall. The comparison of the tangential velocity vector between variations 1 and 2 at the same height shows that the velocity vector in variation 1 is more significant than in variation 2. This tangential velocity produces a rotating flow throughout the drying chamber. That is, variation 1 has a more significant vortex motion than variation 2. This will be seen in the trajectory of the particle.

In Fig. 6 both variations have secondary flows. The secondary flow in variation 1 is clearly visible, after the dry air has completely reached the circular path in the upper chamber. Whereas in variation 2, secondary flow only appears near the inlet due to the collision of dry air against the middle wall. In variation 2, adjacent streams are pulled by an imaginary force to tend to lean to the right side of the chamber, as shown in Fig. 8. This illustrates that the product will accumulate on the right side of the drying chamber.

Fig. 8 shows a comparison of variations 1 and 2 in the trajectory of the spray nozzle particles. In variation 1, it can be seen that the trajectory of the spray nozzle particles has a more significant circular motion than the second variation. The increase in the tangential velocity of the intake air increases the velocity increase which is due to the increase in residence time. The increase in the evaporation rate in the drying chamber is due to the particle trajectory following the air flow which has a tangential velocity, so that larger particles remain, which means greater evaporation time. Meanwhile, variation 2 has a smaller tangential velocity than variation 1, thereby reducing circular motion. As a result, the amount of drying product is less, and the residence time will be faster.

A more uniform temperature contour is seen in variation 1 than in variation two in Fig. 8. Smaller resistance in the axial direction and a more significant circular motion is shown in variation 1. Axial velocity and circular motion are more remarkable in variation 1, favoring the mixing process. between dry air and a more even nozzle spray.

While the temperature contour of variation 2 is not uniform because of the dry air resistance in the axial position and small circular motion. The effect is on the uneven mixing process. This means that the tangential velocity has a significant effect on the mixing process at the radial position. In addition, the impact of the collision between dry air and the middle wall in variation 2 other than as a flow blocker, secondary flow appears near the inlet which tends to lead to the right side of the drying chamber.

In Fig. 8 shows the comparison of the chamber temperature distribution along the y direction between variations 1 and 2, that the temperature variation 1 increased significantly than variation 2. This implies that the quality of the mixture between the spray nozzle and the dry air is well mixed at variation 1. The material receives The hot air is simultaneously and gradually degraded according its distance from the drying heat source, i.e. at the top of the drying chamber. Air and materials will be separated in the cyclone chamber. High temperatures result in better heat transfer near the nozzles seen at nodes 3 and 4. The effect of a strong vortex will be better to promote drying near the spray so that it can be retained longer at nodes 3, 4 and 5. Particle agglomeration begins at point 3 and at the next node crystallization of product growth occurs. The re-entrained particles from the unit at high velocity are indicative of continuous flow and thereafter the particle temperature becomes constant at node 10.

The novelty of this simulation is the use of a spray dryer machine with a combination of

heating from the heater and exhaust heat from the condenser in the refrigeration system.

So it is very clear that Variation 1 is more recommended than variation 2. The limitation of this study lies in the number of inlets into the spray dryer which is only one channel. In the future research can be done with two or three drying air ducts that enter the drying chamber. So that there is a centrifugal effect that can collide with each other in the middle of the drying chamber and can minimize the occurrence of splashes of liquid material to the edge of the drying chamber. But of course the numerical analysis will be more complex.

4. Conclusions

Contour and velocity vector simulations of both positions of the drying air inlet in the drying chamber show the tangential velocity of the drying air flow. Variation 1, which shows a greater increase in the tangential velocity of the incoming air, this of course will result in a greater increase in the evaporation rate as well, in spray dryer. Temperature variation 1 increased significantly than variation 2. This implies that the quality of the mixture between the spray nozzle and the dry air is well mixed. However, getting further away from the heat source, temperature variations 1 and 2 lead to the same pattern, namely, a decrease in temperature at node 10.

21605

ORIGINALITY REPORT

11%	4%	10%	2%
SIMILARITY INDEX	INTERNET SOURCES	PUBLICATIONS	STUDENT PAPERS

PRIMARY SOURCES

1	Varzakas, Theodoros, and Constantina Tzia. "Dehydration: Spray Drying—Freeze Drying", Contemporary Food Engineering, 2015. Publication	2%
2	E. Kavak Akpinar, A. Midilli, Y. Bicer. "Energy and exergy of potato drying process via cyclone type dryer", Energy Conversion and Management, 2005 Publication	1%
3	"Handbook of Drying for Dairy Products", Wiley, 2017 Publication	1%
4	Lixin Huang, Arun S. Mujumdar. "Development of a New Innovative Conceptual Design for Horizontal Spray Dryer via Mathematical Modeling", Drying Technology, 2005 Publication	1%
5	Ankur Kumar, Jyeshtharaj B. Joshi, Arun K. Nayak, Pallippattu K. Vijayan. "3D CFD simulations of air cooled condenser-III:	1%

Thermal–hydraulic characteristics and design optimization under forced convection conditions", International Journal of Heat and Mass Transfer, 2016
Publication

6	Chang Su, Johan Dalgren, Björn Palm. "High-resolution mapping of the clean heat sources for district heating in Stockholm City", Energy Conversion and Management, 2021 Publication	1 %
7	Peter Bengtsson. "Experimental Analysis of Low-Temperature Bed Drying of Wooden Biomass Particles", Drying Technology, 2008 Publication	1 %
8	Computational Fluid Dynamics Applications in Food Processing, 2013. Publication	1 %
9	www.researchgate.net Internet Source	1 %
10	www.mdpi.com Internet Source	<1 %
11	M. Mezhericher, A. Levy, I. Borde. "Droplet–Droplet Interactions in Spray Drying by Using 2D Computational Fluid Dynamics", Drying Technology, 2008 Publication	<1 %
12	www.hbni.ac.in	

	Internet Source	<1%
13	dspace.lboro.ac.uk Internet Source	<1%
14	Submitted to Loughborough University Student Paper	<1%
15	Misha, S., S. Mat, M.H. Ruslan, E. Salleh, and K. Sopian. "Performance of a solar assisted solid desiccant dryer for kenaf core fiber drying under low solar radiation", Solar Energy, 2015. Publication	<1%
16	Submitted to University Tun Hussein Onn Malaysia Student Paper	<1%

Exclude quotes	Off	Exclude matches	< 17 words
Exclude bibliography	Off		